

 Open access • Book Chapter • DOI:10.1016/B978-0-12-409548-9.10375-6

Land Surface Temperature — Source link

Zhengpeng Li, Si-Bo Duan

Published on: 01 Jan 2013

Related papers:

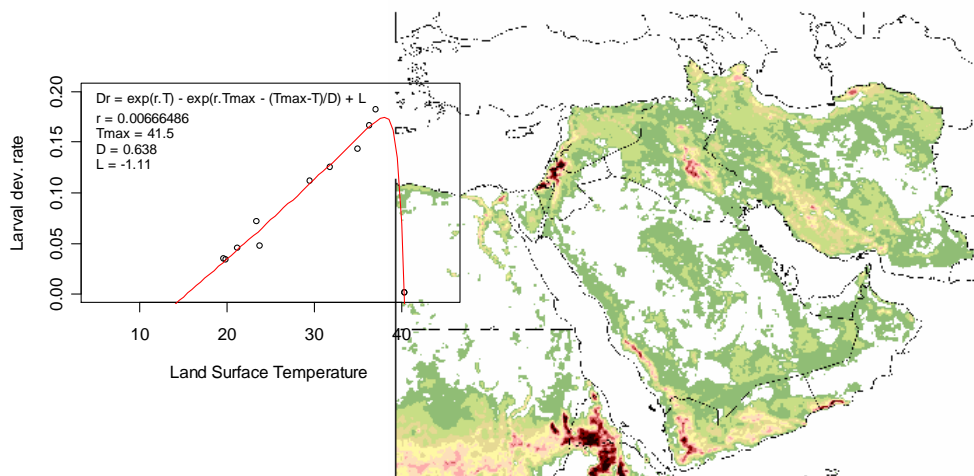
- [Evaluating and improving simulations of diurnal variation in land surface temperature with the Community Land Model for the Tibetan Plateau.](#)
- [Two-Stage Trapezoid: A New Interpretation of the Land Surface Temperature and Fractional Vegetation Coverage Space](#)
- [Control Of Irrigation By Following The Water Balance From Noaa-avhrr Thermal Ir Data](#)
- [Land surface parameterization and modeling over desert](#)
- [A Framework for Coupled Estimation of Evapotranspiration and Recharge Flux by Assimilating Remotely Sensed Land Surface Temperature and Soil Moisture Observation](#)

Share this paper:    

View more about this paper here: <https://typeset.io/papers/land-surface-temperature-48gqrdy7mc>



Geospatial demarcation of Old World Screwworm risk in the Middle East, an update.



March 2008

Dr M. Gilbert

Biological Control and Spatial Ecology
CP160/12 Université Libre de Bruxelles
Av F.D. Roosevelt 50
B-1050 Brussels, Belgium
Email: mgilbert@ulb.ac.be

Dr Jan Slingenbergh

Animal Health Division
Food and Agriculture Organization of the
United Nations (FAO),
Viale delle Terme di Caracalla
00100, Rome, Italy

Table of content

Background & rationale.....	2
OWS Data & identification of the main eco-climatic factors	3
Distribution of OWS cases	3
Vegetation	6
Temperature.....	6
Temporal model.....	9
Spatio-temporal model.....	9
Climate data.....	10
Adjusting the model to LST data	10
Spatial model	12
Spatial extrapolation.....	13
Discussion.....	15
References	16

Background & rationale

This work revises and extends the results presented in a previous study on the same subject carried out in early 2005. The current, improved version accounts for the non-linear relationships between both the development rate of the insect larvae, and the mortality rate of the adults, and temperature. In addition, this study applies a new method of extrapolating the model results obtained for Iraq to the Arabian peninsula.

The persistence of the Old World Screwworm (OWS) *Chrysomya bezziana here*, in areas of endemicity, and its recent invasion into Yemen call for a careful evaluation of the respective risk factors involved.

OWS, to successfully develop, requires warm and wet conditions and is sensitive to prolonged cold or dryness (Sutherst *et al.* 1989). For most of the Middle East, the risk of attracting OWS has been characterized as generally low, using CLIMEX, a climate matching model (Sutherst *et al.* 1989). However, at a more local level, climatic conditions may nevertheless present suitable reproduction conditions for several OWS fly generations and thus support the onset of epidemics. This occurred in parts of the Mesopotamia Valley in Iraq during 1996 to 1998 (Al-Izzi *et al.* 1999; Siddig *et al.* 2005). This example highlights the fact that coarse, large-scale modelling approaches may miss out on locally suitable pockets.

Two other approaches have been applied to quantify the risk of OWS population build up. A growth index model and a life-cycle model were coupled to predict the risk of OWS spread in northern Australia (Atzeni *et al.* 1994). However, this approach simply quantified the spread of OWS in an area already identified at risk using CLIMEX, i.e. tropical and subtropical northern Australia grazing region, and can therefore hardly be used as such to predict the spread of OWS under the dry and harsh conditions of Iraq. Prof. David Rogers explored an alternative approach at the time of the 1996-1998 epidemics, and produced an OWS risk map based on a statistical model relating OWS presence to satellite derived climatic data and measures of their seasonality (Rogers 1997). This approach provided an excellent fit to the observed data set, and assisted the fight against OWS in Iraq but turned of limited use when extrapolating the predictions to other areas because the actual, causal relationship between OWS and the climatic predictors had not yet been uncovered. In other words, some of the statistical associations used in the model may be fortuitous, regardless of their statistical significance in the model, and hence lead to hazardous predictions outside the period and area covered by the training set.

This study aims to revisit the data set of georeferenced OWS outbreaks in Iraq in 1997 using a modelling approach based on biological features modulated by climatic and environmental variables. This increases the chances of obtaining realistic predictions for the period and area outside

the training set, i.e. relevant to other countries in the Middle East.

OWS Data & identification of the main eco-climatic factors

Distribution of OWS cases

OWS introduction and subsequent outbreaks have been reported a number of times in the Middle East (reviewed in Siddig *et al.* 2005) but only translated into important population development in the Sultanate of Oman in 1983 (Spradbery *et al.* 1992), Iran in 1995 (Navidpour *et al.* 1996), and Iraq in 1996. OWS was first reported in Iraq in June 1996 (Abdul Rassoul *et al.* 1996), and the monthly incidence showed two major peaks, respectively in the winters of 1996 and 1997, until 1998 when insecticide formulations became finally available to the veterinary clinics and the incidence reduced (Fig.1). There is evidence to suggest that OWS may have persisted in Iran and Iraq ever since the mid-1990s.

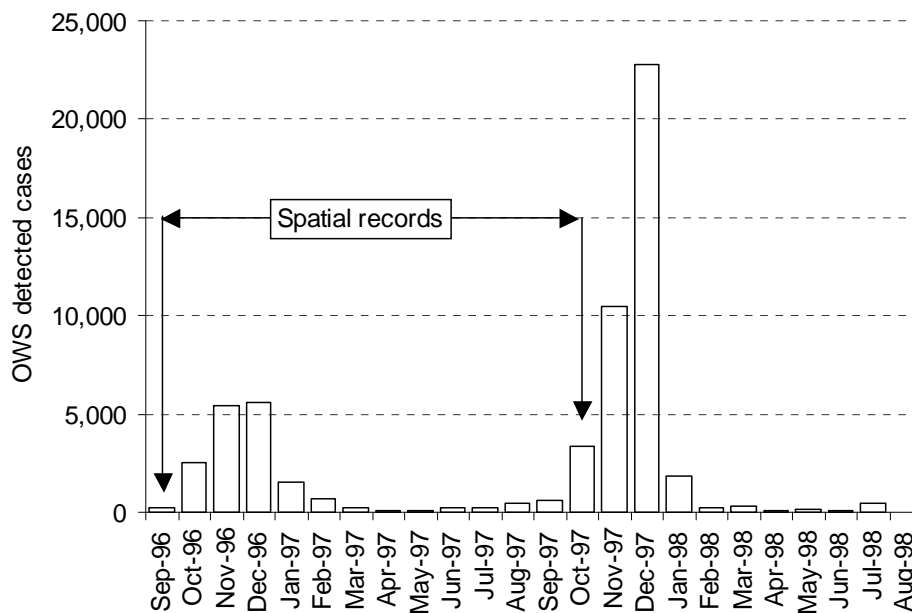


Fig. 1. Monthly OWS detected cases in Iraq from September 1996 to August 1998 (from Siddig *et al.* 2005)

As illustrated in Fig. 1 the geographic distribution of OWS clinical cases was only recorded for the period September 1996 to October 1997 (Oct. 97 is incomplete). OWS cases were grouped by clinic, and assigned to the location of each clinic. However, for the statistical and biological models, these cases could not be assigned to these locations as such, i.e. these cases were not truly *observed* in

these points. It was thus necessary to assign these cases to areas so that an average number of cases by pixel could be estimated and matched against the climatic and environmental predictors. This required redistributing the cases according to areas, and these areas were defined using Thiessens' polygons delimited within each of the provinces that reported OWS cases (Fig.2a). Some of the Thiessens polygon included large areas of desert and water, and those areas were therefore excluded (Fig. 2b). Desert areas were defined as those where the length of growing period was equal to 0 (Wint *et al.* 2005). Detected cases were distributed by polygon, which allowed the production of monthly distribution maps of OWS case densities (Fig. 3). These latter data formed the training set for the spatio-temporal population model.

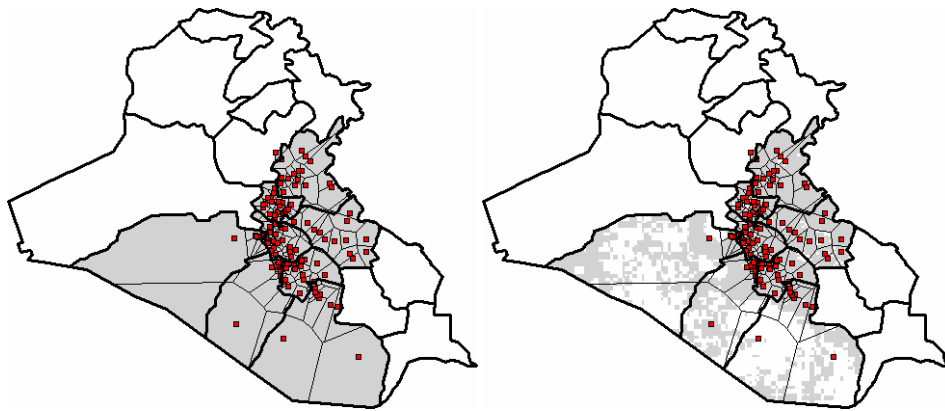


Fig. 2. (a) Left. Distribution of clinics reporting OWS data (presence or absence; red dots), and the Thiessens's polygon for each point (light grey polygon). (b) Right. Same as (a), but excluding deserts and lakes from each clinic covered area.

The spatio-temporal distribution shows that OWS monthly cases occurred fairly widespread in the study area during the initial study period, with an expansion in Nov-Dec, and, next, a significant decrease. Very few isolated cases persisted in a few areas only, in later spring/summer. OWS flared up again in the autumn of 97. In April 97, OWS was almost stuttering to extinction, as the disease persisted in two isolated foci; one wonders whether OWS had persisted at a very low incidence also in some other areas.

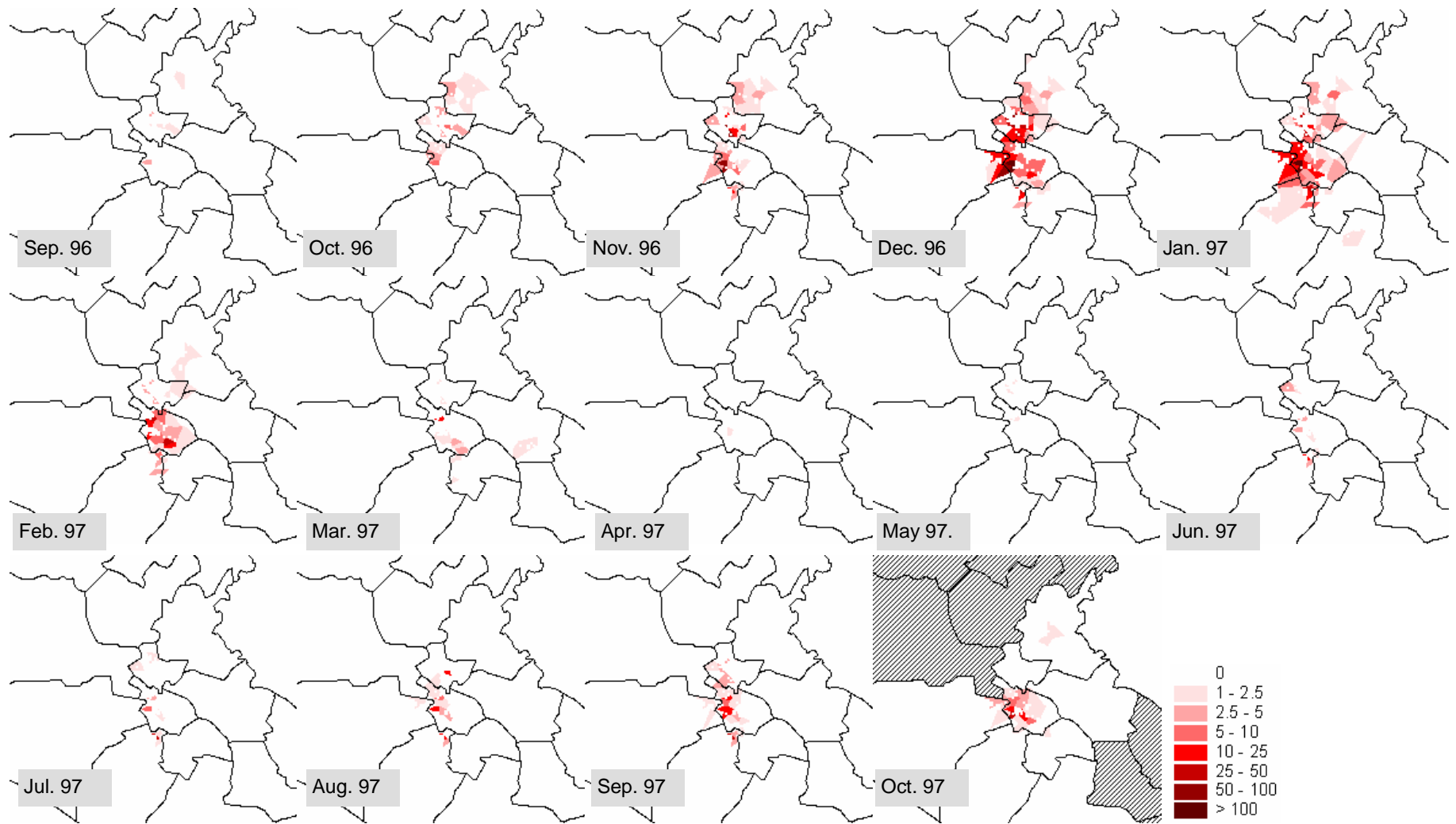


Fig. 3. Monthly distribution of OWS case density (cases per 0.05 decimal degree pixel) from Sep. 1996 to October 1997 in Iraq.

Vegetation

Given its sensitivity to prolonged dryness, OWS meets with rather adverse climate conditions over large areas of Iraq but may persist in areas with enough moisture and shade. Actually, the vast majority of OWS cases have been observed in or near areas with some vegetation (Fig. 4). This corroborates with the observation that OWS adults tend to avoid flying in desert and arid areas.

This is a very important feature in the risk assessment of OWS because areas with dense enough vegetation may readily be identified by remote sensing, using the normalised difference vegetation index (NDVI).

NDVI is an index derived from the reflectance measured by satellite sensors in the red and infra-red portions of the light spectrum (NASA 2005). Reflectance in the red region decreases with increasing chlorophyll content of the plant canopy, while reflectance in the infrared increases with increasing wet plant biomass. The NDVI is thus a “greenness” index that measures both vegetation presence and growth conditions (Cihlar *et al.* 1991).

The NDVI index may be obtained for large areas and the association OWS presence and minimal NDVI threshold is presumably rather stable and may be realistically extrapolated for other areas. In other words, the NDVI association enables production of a large-scale mask to depict areas that may be suitable for OWS development.

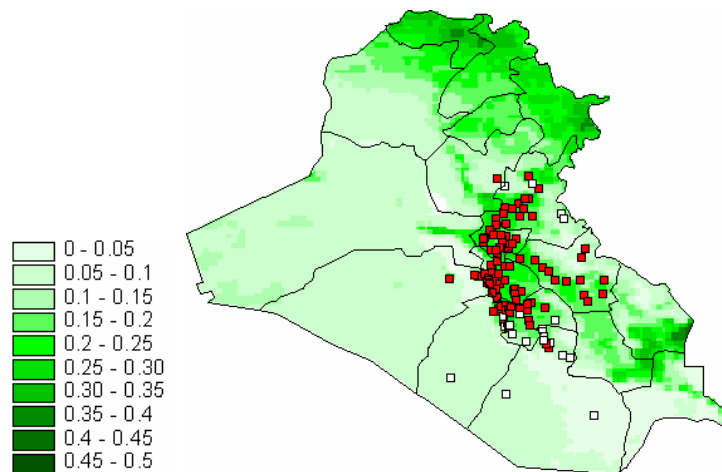


Fig. 4. Distribution of clinics that reported OWS cases (red dots), and those without a single case detected (white dots) over the distribution of NDVI.

Temperature

Another critically important factor is temperature: OWS reproduction is constrained by cold and extreme hot conditions, both resulting in high mortality rates. This information may be applied in order to determine which area presents the right sequence of a mild winter and relatively cold summer so as to allow OWS persistence and spread.

The effect of temperature on two important life cycle stages was studied by Siddig *et al.* (2005): larval development duration (days), and adult longevity (days) were assessed as a function of temperature. Modelling the development rate of insect larvae as a function of temperature is a classical problem in entomology, which has been addressed by several models, which are presented in detail in Rabinovich *et al.* (2006). From the four model presented in this analysis, we retain the standard linear model, and the non linear Lactin model which account for lethal high temperature. For the linear model, we obtained the best-fit model illustrated in Fig. 5 (a). However, revisiting the paper by Siddig *et al.* (2005), we find that no larvae emerged during July and August, when monthly average temperatures surpassed 30°. So this adds two points to the plot, both with a larval development rate equal to zero, that we can use to fit a Lactin model illustrated in Fig. 5 (b), which account for the negative effect of both low and high temperatures on larval development.

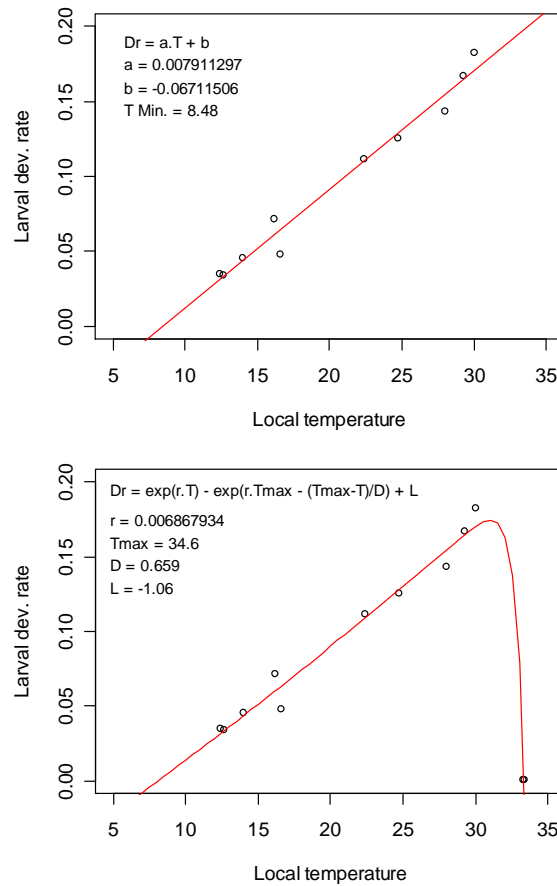


Fig. 5. Models of larval development rate as a function of temperature, using a linear and Lactin model.

Modeling the adult fly mortality rate as a function of temperature can be carried out using a variety of non-linear functions. Four models were tested and are presented in Fig. 6. We note the best-fit is obtained for model 4, assuming a relatively constant mortality rate of adults for mean average temperatures up to

around 20°, followed by a moderate decrease in longevity as monthly average temperature rises. This model predicts 100% mortality at temperature = 38.50°C, whilst Model 1 predicted 100% mortality at 35.49°C.

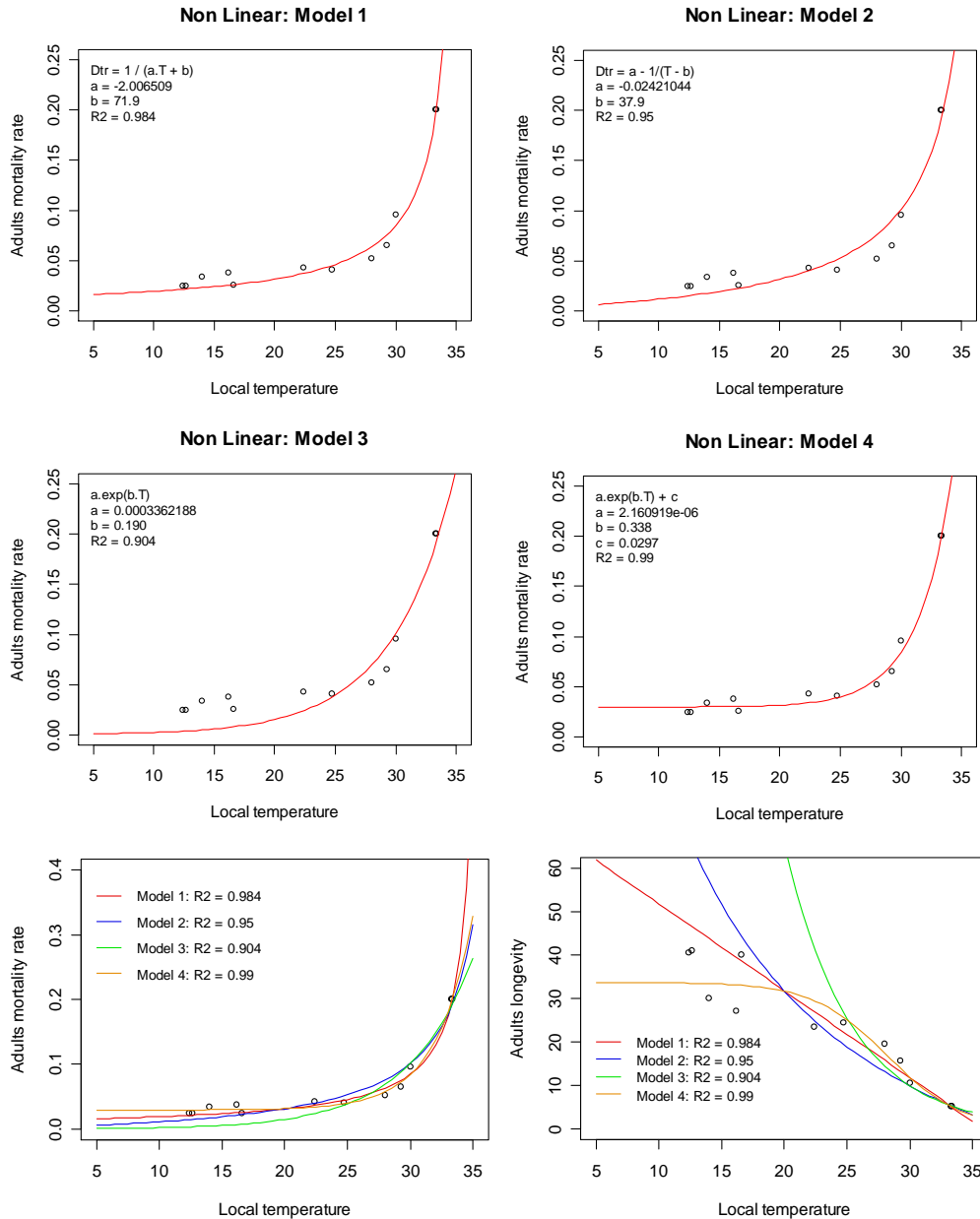


Fig. 6. Models of adult mortality rate as a function of temperature.

The use of Lactin model of larval development rate, and the above Model 4 for adult fly mortality are henceforth applied in the analyses.

Temporal model

A first, temporal model aims to establish if the relationship between respectively (i) larval development rate, and (ii) adult longevity, and temperature can be applied to explain the change of OWS cases in time (as shown in Fig. 1) using monthly temperature records from Baghdad, Iraq. The dependent variable was the number of OWS cases per month from Sep. 96 to Jan 98, when veterinary control by insecticides became important. Average temperature records were obtained for Baghdad from the “Global Historical Climatology Network” (<http://www.worldclimate.com>). At each time step, the number of OWS cases was estimated as:

$$N_{t+1} = N_t \cdot R_n \text{ (Eq. 1)}$$

$$R_n = C_{f1} \cdot Dev - C_{f2} \cdot Dth \text{ (Eq. 2)}$$

$$Dev = f(T^\circ) \text{ (see Lactin Model in Fig. 5)}$$

$$Dth = f(T^\circ) \text{ (see Model 4 in Fig. 6)}$$

where N_{t+1} is the number of cases at time step + 1, N_t is the number of OWS cases in the previous time step, Dev and Dth are the development rate and death rate respectively established from their relationship with temperature (Fig. 5b, and Fig. 6), and C_{f1} and C_{f2} are two correcting factors accounting for all other effects ignored in this simplified model. C_{f1} and C_{f2} were estimated such as to minimise the sum of squared difference between the observed and modelled number of cases. A lag of one month was applied to account for the delay between actual OWS case development and date of reporting (Fig. 7).

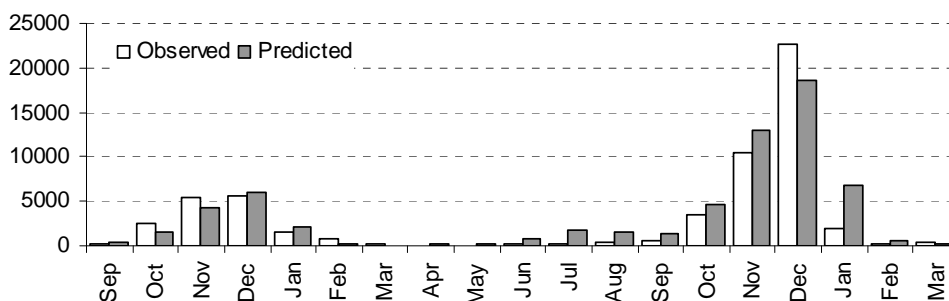


Fig. 7. Observed and predicted number of OWS cases with a 1-month lag ($R^2 = 0.89$, $C_{f1} = 23.2$, $C_{f2} = 3.94$, $N_0 = 458$).

The result illustrated in Fig. 7 demonstrates that the seasonality in OWS records is captured simply by taking into account the role of temperature on larvae development rate and adult longevity.

Spatio-temporal model

Building the spatio-temporal model of OWS in Iraq involved several additional steps: i) pre-processing

satellite-derived data on the distribution of temperature and NDVI, *ii*) adjusting the model to account for the distribution of temperature and NDVI, and *iii*) searching for the best-fit parameters.

Climate data

Data on the distribution of temperature were obtained from the weather satellites NOAA, following the procedure detailed in Bieseman (2001). The NOAA data archive was searched for all images intercepting a rectangle delimitating the study area (Fig. 7), taken between the 1st of August 1996 and the 1st of February 1998, at a time comprised between 7:00 and 15:00 UTC. This query resulted in 3,402 images for a total of 10.0 GB of downloaded data. These data were subject to geometric corrections, and used to compose monthly cloud-free images of land surface temperature (LST) as defined by Price (1984) as

$$T = Ch4 + 3.33 (Ch5 - Ch4) \text{ (Eq. 4)}$$

and normalised difference vegetation index (NDVI) defined as

$$NDVI = (Ch2 - Ch1) / (Ch2 + Ch1) \text{ (Eq. 5)}$$

where Ch1, Ch2, Ch4 and Ch5 are the values taken by the different channel instruments.

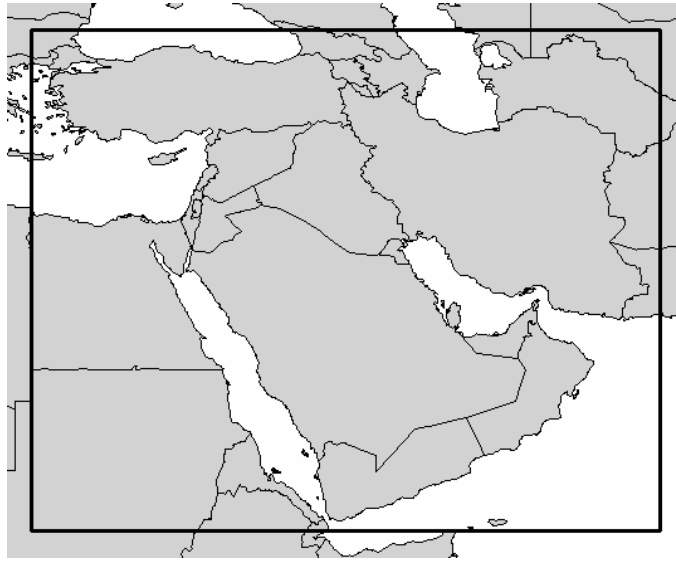


Fig. 7. Area selected for the extraction of AVHRR climate data.

Adjusting the model to LST data

The model predicting larvae development and fly mortality rates was based on local temperature. However, we wanted to apply this model at a broad-scale, using LST temperature estimates, which do not exactly match the locally measured temperature. Therefore, we re-scaled local temperatures in LST, using the linear regression presented in Fig. 8. The LST-rescaled temperature were then used to predict larval development rate and adult mortality rate, using similar models, but providing with different best-fit parameters illustrated in Fig. 9.

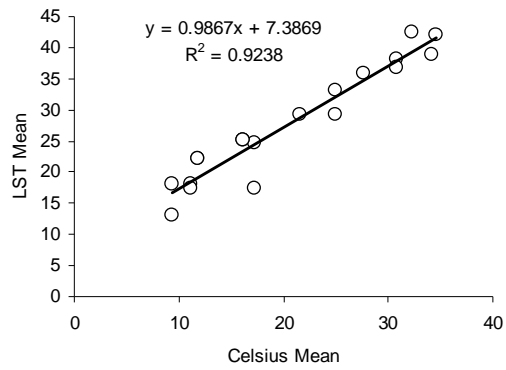


Fig. 8. Land Surface temperature monthly mean as function of local monthly means temperature measured in Baghdad.

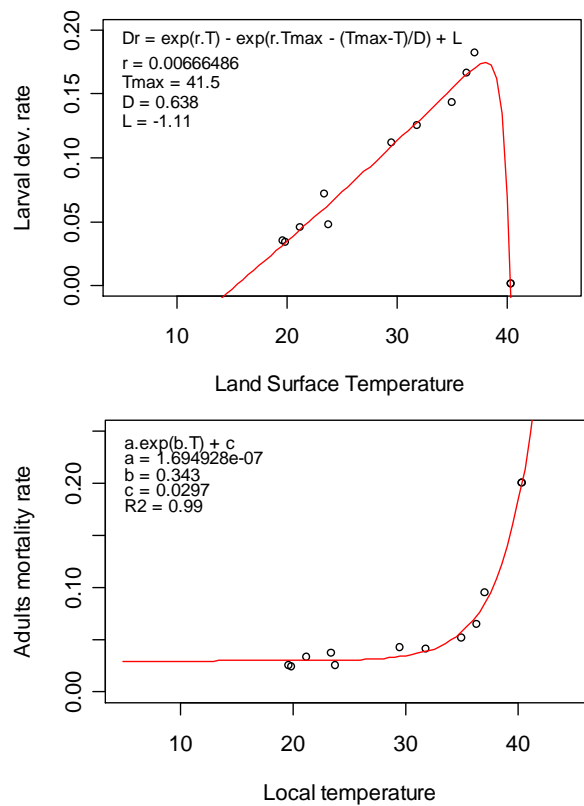


Fig. 9. Larval development rate and adult mortality rates expressed as a function of LST-rescaled temperature (°C).

These updated predictions served to model the epidemic curve of monthly OWS cases using the model described in Eq. 1 & 2. The resulting predictions are illustrated in Fig. 10. The model best-fit parameters yield an overall net monthly OWS reproduction rate illustrated in Fig. 11.

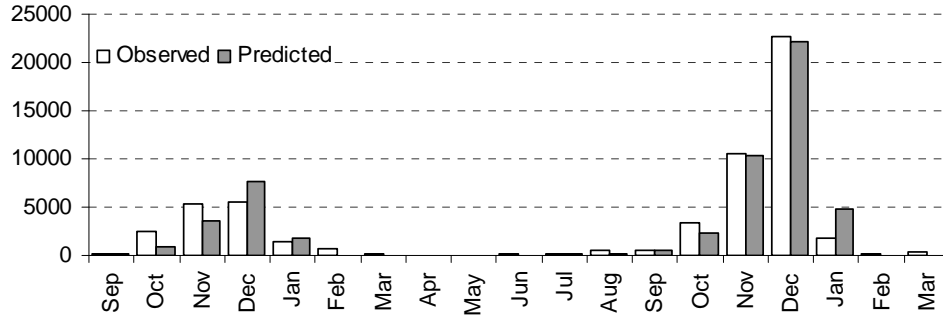


Fig. 10. Observed and predicted number of OWS cases with a 1-month lag, based on LST-rescaled model ($R^2 = 0.95$, $C_{f1} = 41.4$, $C_{f2} = 23.13$, $N_0 = 163$).

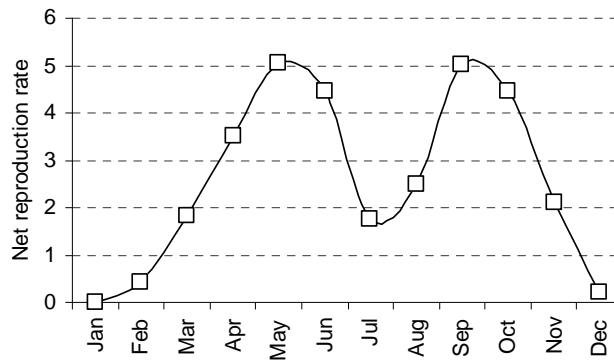


Fig. 11. Change in the net reproduction rate estimated from the best-fit parameters using LST-rescaled temperature predictions of development and mortality rate.

This model has even a better fit than the one using temperature measured on the ground, indicating that there was no loss in predictive power resulting from the re-scaling into temperature measurements derived from satellite imagery data.

Spatial model

The best-fit parameters identified in the model illustrated in Fig. 10 were used to derive the monthly spatial distribution of the net reproduction rate as a function of temperature. For each cell of the study area illustrated in Fig. 7, we estimate the summed monthly net reproduction rates, for a full calendar year, as an indicator of the local suitability for OWS population build up. Using the training set of OWS outbreak locations in Iraq, we established a multiple logistic regression model where OWS presence/absence was predicted as a function of NDVI (NDVI² to account for non-linear relationship), SumRn, the summed reproduction rate over the 12 calendar months, and the interaction between NDVI

and SumRn. The model was established to apply to the pixel level, to be able to readily compute the predicted OWS risk for the entire study area, based on the available imagery data. This result is an inflated number of degrees of freedom, because the OWS records by each veterinary clinic have been converted into densities, covering multiple pixels. However, since the primary aim here is to predict rather than to infer, this should not affect the results aimed for. Still, the very high level of significance shown for the different terms (Table 1) should be interpreted with caution. OWS dispersal was accounted for by smoothing the prediction results using a Gaussian redistribution kernel that assumes a random diffusion of the flies. The multiple logistic regression results are presented in Table 1. The model attains an overall accuracy of 80.4% and an area under the ROC curve of 0.697, which can be considered as a moderate to good level of prediction.

Table 1 Multiple logistic regression statistics for the presence/absence of OWS as predicted by NDVI and RnSum, the summed OWS net reproduction rate over a calendar year.

	Estimate	Std. Error	z value	Pr(> z)
(Intercept)	0.588	0.254	2.313	0.0207 *
Ndvi	-27.86	2.115	-13.17	<0.001 ***
Ndvi2	-68.64	4.897	-14.01	<0.001 ***
SumRn	-0.0944	0.00822	-11.47	<0.001 ***
Ndvi:SumRn	1.462	0.0604	24.20	<0.001 ***

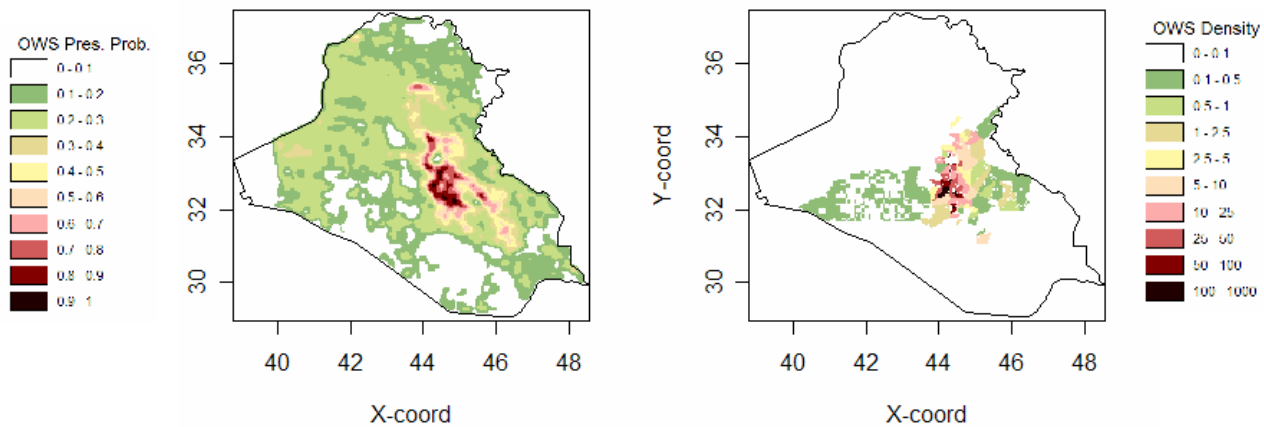


Fig. 12. Predicted probability of OWS presence (left) and OWS observed density (right, cases per 0.05 decimal degree pixel).

Spatial extrapolation.

The two key variables included in the model are directly and explicitly related to the OWS life cycle, and are therefore believed to apply to the (potential) OWS distribution outside the area used to build the model. The spatial distribution of the two key variables NDVI and SumRn is shown in Fig. 13. The model prediction

is illustrated in Fig. 14. It is recalled that these extrapolation represents the risk of persistence and local developments if OWS were introduced in a given area.

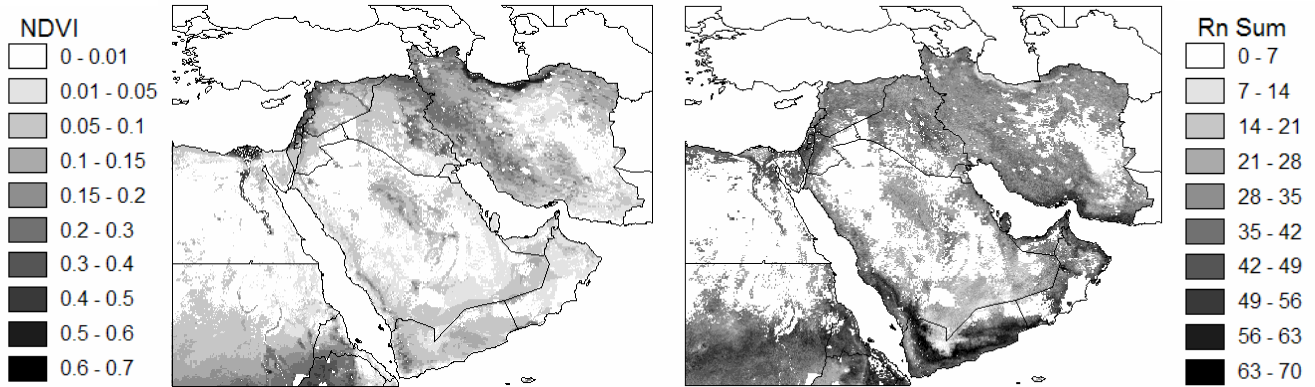


Fig. 13. Distribution of NDVI and of the calendar year sum of monthly net OWS reproduction rate derived from LST.

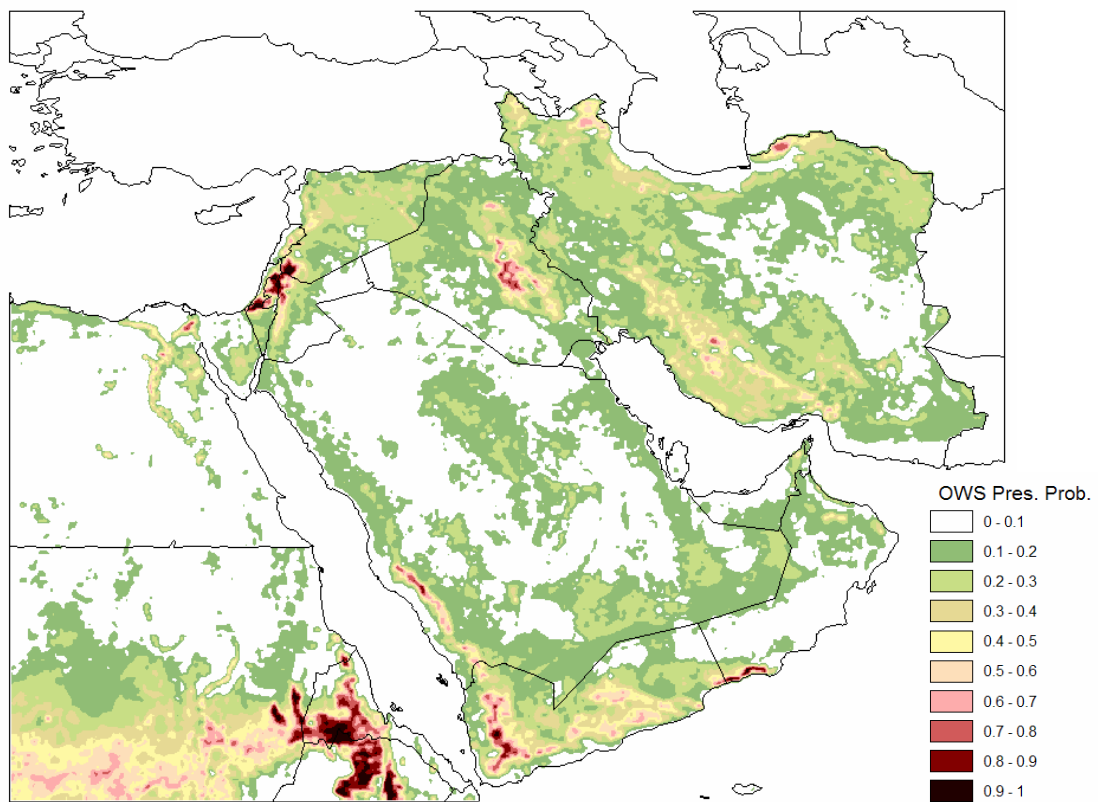


Fig. 14. Distribution of predicted OWS probability in the study area, based on eco-climatic suitability.

This layer of OWS presence probability can be multiplied by the density of livestock unit (Bovine = 0.7 unit, Sheep = 0.1 unit, Goat = 0.1 unit) in order to derive an index of risk for the prevailing livestock, as illustrated

in Fig. 15.

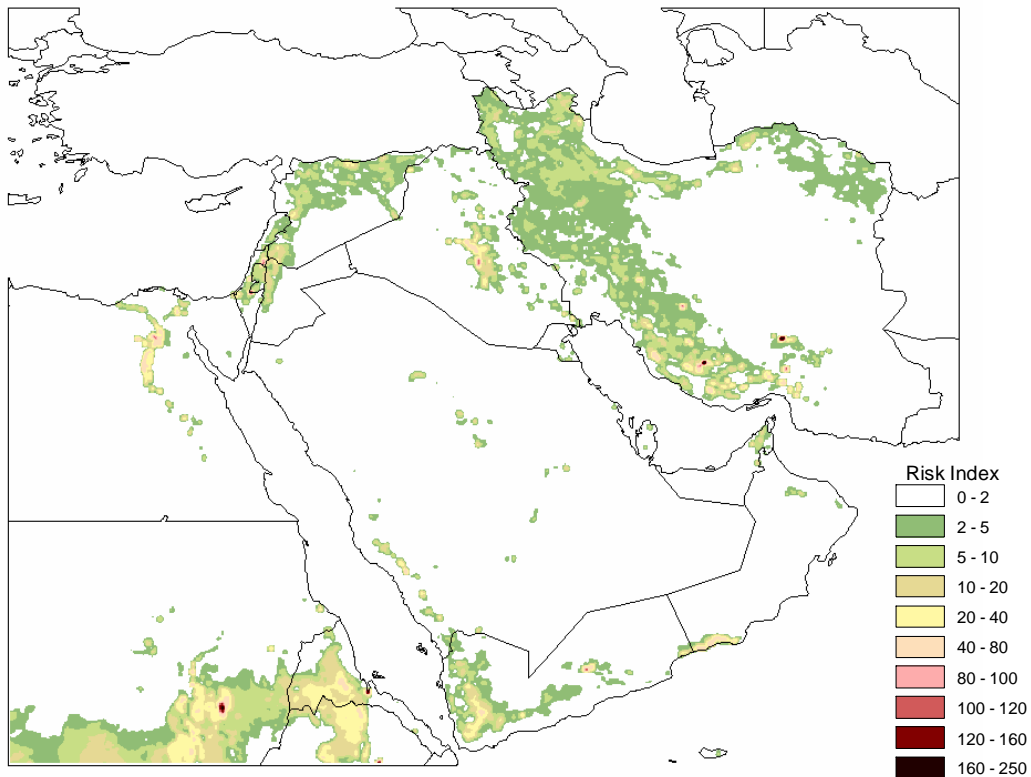


Fig. 14. Distribution of predicted OWS risk for livestock in the study area, based on eco-climatic suitability.

Discussion

The large scale display of the OWS risk prediction for the Middle East/Arabian Peninsula depicts relatively few areas identical to that of the Mesopotamia Valley and suited for OWS permanence/development. The risk areas identified include a few hotspots in southwest Iran, southwest Yemen, and along the south coast of Oman. Suitable condition areas are also observed in parts of Syria, Lebanon, Jordan, Israel, along the Nile valley in Egypt and in relatively large areas of Eritrea, Ethiopia and Sudan. The delineation or demarcation of these areas might be somewhat too restrictive, given that the much larger area that appears to be suitable on the basis of temperature alone (Fig. 12 right). Thus, it is very well possible that OWS may locally persist also in parts of Saudi Arabia, several Gulf countries and inland Oman.

There are two main reasons to remain somewhat cautious when interpreting the risk map illustrated in Fig. 14. First, the map is based on a model developed using Iraq data only, extrapolated to predict the risk for a much wider area, under the assumption that OWS biology and dependency on temperature and vegetation applies everywhere and in the same manner. One should be aware of this assumption when reading the map as the best predictions are expected for countries sharing an Iraq type

climate.

Second, most of the Middle East landscape shows a vegetation pattern heavily dependent on water availability and therefore subject to rapid anthropogenic change. Even when global climate change becomes reality, the change in temperature is rather slow compared to the dynamic hydrology and land use pattern. A recent example is the restoration of wetlands in the marshland of Mesopotamia, (Nature 2004). Thus, if we take the relatively large temperature-suitable area defined in Fig. 12, it follows that any change in moisture, vegetation and shade could greatly alter the local risk of OWS persistence. The prediction based on temperatures therefore serves as a background OWS suitability mask, to be viewed in conjunction with the dynamic distribution of vegetation and the hydrological and land use patterns.

It remains that the areas in the Arabian peninsula predicted as high risk areas call for special attention. Follow-up is indicated in order to collect more data on OWS in high risk settings and relate the local OWS risk to the corresponding ecoclimatic setting. The recent outbreaks in western parts of Yemen confirm that the OWS distribution in the Middle East remains fluid.

References

- Abdul Rassoul, M.S., Ali, H.A. & Jassim, F.A. (1996) Notes on *Chrysomya bezziana* Villeneuve (Diptera: Calliphoridae), first recorded from Iraq. *Bulletin of the Iraq Natural History Museum*, **8**, 113–115.
- Abo-Shehada, M.N. (2005) Incidence of *Chrysomya bezziana* screw-worm myiasis in Saudi Arabia, 1999/2000. *Veterinary Record*, **156**, 354-356.
- Al-Izzi, M.A.J., Al-Taweel, A.A. & Jassim, F.A. (1999). Epidemiology and rearing of Old World Screw-worm, *Chrysomya bezziana* (Villeneuve) Diptera: Calliphoridae in Iraq. *Iraqi Journal of Agriculture*, **4**, 160-153.
- Al-Jowary, S.A.K. (2000) *Study of the effect of some environmental factors on the biology of the Old World Screw-worm Fly, Chrysomya bezziana Villeneuve, (Diptera: Calliphoridae)*. M. Sc. Thesis, College of Education for Women, University of Baghdad (In Arabic).
- Atzeni, M.G., Mayer, D.G. Spradbery, J.P., Anaman, K.A. & Butler, D.G. (1994) Comparison of the predicted impact of a screwworm fly outbreak in Australia using a growth index model and a life-cycle model. *Medical and Veterinary Entomology*, **8**, 281–291.
- Bieseman, J. (2001). *Seasonality Mapping of Climatic and Vegetation indices in the Eurasian Ruminant Street*. Report to the Food and Agriculture Organization of the United Nations, Agah, pp. 43.
- Cihlar, J., St-Laurent, L. & Dyer, J.A. (1991) Relation between the normalized vegetation index and ecological variables. *Remote Sensing of Environment*, **35**, 279-298.
- Hall, M.J.R., Edge, W., Testa, J., Adams, Z.J.O. & Ready, P.D. (2001) Old World screwworm fly, *Chrysomya bezziana* occurs as two geographical races. *Medical and Veterinary Entomology*, **15**, 1-11.
- Navidpour, Sh., Hoghooghi-Rad, N., Goodrazi, H. & Pooladgar, A.R. (1996) Outbreak of *Chrysomya bezziana*

- in Khoozestan province, Iran. *Veterinary Record*, **139**, 217.
- Nature (2004) Cash floods in to save Iraq's Garden of Eden. *Nature*, **496**, 430.
- NASA (2005). NASA earth observatory: Glossary. http://eobglossary.gsfc.nasa.gov/glossary_mode.html (visited in March 2005)
- Price, J.C. (1984) Land surface temperature measurements from the split window channels of NOAA-7 Advanced Very High Resolution Radiometer. *Journal of Geophysical Research*, **89**, 7231-7237.
- Rabinovitch, J., Pietrokovsky, S. & C. Wisnivesky-colli (2006) Temperature and development rate of *Triatoma guasayana* (Hemiptera: Reduviidae) eggs under laboratory conditions: physiological and adaptive aspects. *Physiological Entomology*, **31**:361-370.
- Rogers, D.J. (1998) Risk maps for Old World Screwworm in the Middle East. Report on a mission to the Republic of Iraq for the Food and Agriculture Organization of the United Nations, FAO project codes TCP/IRQ/6611(E) and OSRO/IRQ/701/NET, pp. 21.
- Siddig, A., Al Jowary, S., Al Izzi, M., Hopkins, J., Hall, M.J.R. & Slingenbergh, J. (2005) Seasonality of Old World Screwworm myiasis in the Mesopotamia valley in Iraq. *Medical and Veterinary Entomology*, **19**:140-150.
- Spradbery, J.P., Mahon, R.J., Morton, R. & Tozer, R.S. (1995) Dispersal of the Old World Screw-worm Fly, *Chrysomya bezziana*. *Medical and Veterinary Entomology*, **9**, 161–168.
- Spradbery, J.P., Khanfar, K.A. & Harpham, D. (1992) Myiasis in the Sultanate of Oman. *Veterinary Record*, **131**, 76-77.
- Sutherst, R.W., Spradbery, J.P. & Maywald, G.F. (1989) The potential geographical distribution of the Old World screw-worm fly, *Chrysomya bezziana*. *Medical and Veterinary Entomology*, **3**, 273-280.
- Wint, W. (2003) *Food and Agriculture Organization of the United Nations livestock distribution data archive*. Restricted access web hosted data archive prepared by Environmental Research Group Oxford Limited for the Pro Poor Livestock Policy Initiative of the Animal Production and Health Division of the Food and Agriculture Organization of the United Nations, Rome, Italy. Accessed in January 2005 in <http://ergodd.zoo.ox.ac.uk/agaagdat/index.htm>